Magma flow directions in Azores basaltic dykes from AMS data: preliminary results from Corvo island

Direcciones de flujo ígneo en diques basálticos de Azores a partir de datos de ASM: resultados preliminares en la isla de Corvo

Ó. Pueyo Anchuela [1], A. Gil [1], M. Lago [1], Z. França [2] y C. Galé [1]

[1] Departamento de Ciencias de la Tierra. Universidad de Zaragoza. C/Pedro Cerbuna, nº12. CP. 50.009 Zaragoza. opueyo@unizar.es
[2] Departamento de Geociencias, Universidades dos Açores, R. Mare de Deus, 9501-801. Ponta Delgada, Portugal.

RESUMEN

Se presenta el estudio preliminar de flujo ígneo en diques basálticos de la isla de Corvo, (Azores), usando la técnica de la Anisotropía de la Susceptibilidad Magnética (ASM). Las muestras proceden de un total de 5 diques con una orientación variable N-S a NE-SO. Uno de los diques se localiza en la zona central de la caldera volcánica y el resto en la sector meridional de la isla. Todos los diques muestran una fábrica magnética normal determinada por la orientación preferente de cristales de magnetita y caracterizada por una foliación magnética paralela a las paredes. Para el dique localizado en la caldera volcánica, la lineación magnética, en posición vertical, contrasta con la lineación horizontal obtenida en el resto de las estaciones. Estos resultados son compatibles con un modelo de emplazamiento caracterizado por un flujo vertical del magma en la zona central del complejo volcánico que gradualmente se horizontaliza en las zonas distales del complejo.

***Key words**: AMS technique, basaltic dykes, magma flow direction, Corvo Island, Azores.*

Geogaceta, 40 (2006), 83-86
ISSN: 0213683X

Introduction

The Azores archipelago is made up of nine volcanic islands located near the triple junction of the North America, Eurasia and African plates (Fig. 1). Seven of them (the Eastern Islands, located to the East of the Middle Atlantic Ridge) belong to the Eurasian Plate (Forjaz, 1988). The other two (Flores and Corvo) are located to the west of the Mid Atlantic Ridge (Western Islands) and belong to the North American Plate.

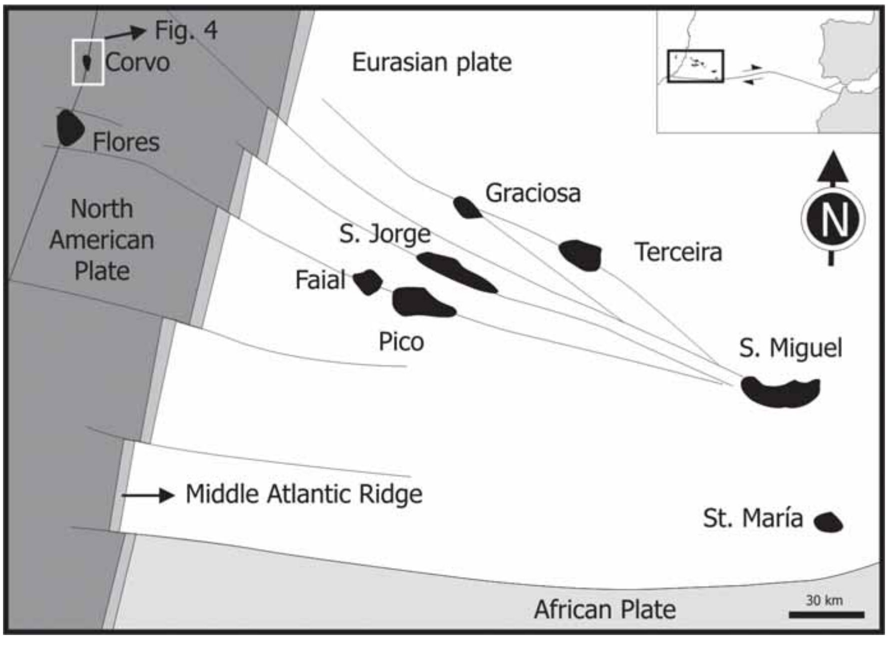

Fig. 1.- Location of the Corvo Island within of the Azores Archipielago (after Forjaz, 1988)

Fig. 1.- Localización de la Isla de Corvo en el Archipiélago de las Azores (Figura modificada de Forjaz, 1988)

The formation and evolution of the Western Islands during Cuaternary times has been related with a set of tectonic structures which are responsible for the present-day seismicity in these islands. In contrast with the Eastern Islands, with WNW-ESE structural trends, the N-S elongation of both Flores and Corvo island, suggest an evolution linked with the Mid Atlantic Ridge dynamics (França *et al*., 2003).

The volcanic history of Corvo Island is characterized by the superposition of several volcanic stages with very differenciated emplacement modalities and lithotypes (França *et al*., 2003). Three main stages are differenciated: 1) Fissural stage linked to submarine volcanic activity and responsible for the proto-island building (shield volcano); 2) Explosive stage characterized by different pyroclastic lithotypes and 3) Effusive and filoniane stage responsible for the complex net of dykes affecting the previous units. The radiometric dating (K-Ar) in materials corresponding to the last stage have revealed a maximun age of around 0.7 M.y. for these rocks (Azevedo *et al.*, 2003).

In this work we present the first results on the magnetic fabric of subvertical dykes at a decametric scale which correspond to the filoniane stage. The main objective of this study is centered on the characterization of kynematic aspects related to the dyke emplacement.

Anisotropy of Magnetic Susceptibilty

Since the magnetic fabric reflects the spatial organization of the magnetic minerals, the anisotropy of magnetic susceptibility (AMS) technique has proved to be a valuable tool for defining both direction and sense of lava flow within tabular intrusions such as dykes and sills (Ellwood, 1978, Rochette *et al.*, 1991; Cañon-Tapia *et al.*, 1996; Geoffroy *et al.*, 2002). Two general models describe the relationship between magma flow direction and principal susceptibility axes in such intrusions. The classical application of the AMS technique to igneous rocks assumes that the magnetic lineation (or the mean of the *K*1 axes) is parallel to the magma flow vector (Knight and Walker, 1988; Rochette *et al.*, 1991; Herrero-Bervera *et al.*, 2001). In the second model, the flow vector is estimated from the geometric computation between the *K*3 axes and the pole of the intrusion wall (Hillhouse and Wells, 1991; Geoffroy *et al.*, 2002), as *K*1 often results in an intersection axis (the zone axis of sub-fabrics).

The anisotropy of magnetic susceptibility (AMS) technique is based on the measurement of the variation of susceptibility in a standard volume of rock when a weak magnetic field ($\leq$ 1mT) is applied in different directions. Such a variation can be described mathematically by means of a second-rank symmetric tensor, which can be physically expressed as an ellipsoid whose principal axes represent the three principal susceptibilities (maximum, intermediate and minimum susceptibility axes, or $K1 \geq K2 \geq K3$). With independence of the source of the magnetic susceptibility (ferromagnetic, paramagnetic or diamagnetic minerals), it has been demonstrated that the magnitude of this anisotropy depends on two factors: the magnetic anisotropy of the particles themselves and the degree of their alignment (Tarling and Hrouda, 1993). The preferred orientation of crystallographic axes (crystalline anisotropy) determines the AMS for the majority of minerals (mainly in paramagnetic minerals and haematite). In the case of magnetite, the AMS is controlled by the shape preferred orientation of individual grains or grain aggregates (shape anisotropy).

Many parameters are classically used to describe the AMS fabric of rocks. In this study we use the following parameters to characterize the magnitude and shape of the susceptibility ellipsoid (Jelinek, 1981; Hrouda, 1982):

Corrected anisotropy degree:
$Pj=\exp[2(h_1-h_m)2+(h_2-h_m)2+(h_3-h_m)2]1/2$

where $h_1 = \ln K_1$, $h_2 = \ln K_2$, $h_3 = \ln K_3$ and $h_m = (h_1+h_2+h_3)/3$

Shape parameter:
$T = [2\ln(K2/K3)/\ln(K1/K3)] - 1$

The P*j* parameter is used to quantify the degree of magnetic anisotropy and T characterizes the shape of the AMS ellipsoid. In addition to these parameters, we also use the bulk magnetic susceptibility $K_m = (K1+K2+K3)/3$.

Results

Samples for the AMS analysis were collected from 5 dykes. One (site COR3) coming from the center of the northernmost caldera and the others from the southern sector of the island (Fig. 2(a)). Two different sampling procedures were carried out. On site COR3 more near to sixty cores were drilled. Part of these come from the central part of the dyke (Fig. 2(b)) and the rest from the two dyke walls (Fig. 2(c)). In the rest of the dykes, blocks oriented to the central part were collected and drilled in the laboratory, later on.

The mesoscopic dykes in the Corvo island show an orientation between N010E to N090E (Fig. 2d), with a main NNE to SSW trend, parallel to the long axis of the island. The thickness of the sampled dykes varies between 0.5 m and 1.5 m.

Magnetic susceptibility and magnetic mineralogy

Bulk magnetic susceptibility ranges from 2×10^{-3} to 40×10^{-3} SI. As can be seen in the *K*m vs P*j* plot (Fig. 3(a)), great differences exist in the *K*m values between samples coming from the dyke located at the center of the northernmost caldera (site COR3) and those of the southern part of the island. These differences can be explained in terms of petrological differences. Samples from site COR3 correspond to a porphyritic basalt with olivine, piroxene and plagioclase phenocrysts with magnetite crystals as the only ferromagnetic phase. The rest of the samples vary from plagioclase-rich to olivine-rich basalts with a higher content in magnetite crystals and a more fluidal rock-texture. In any case all the obtained *K*m values agree with those found in basaltic dykes where magnetite is the main carrier of the susceptibility (Hrouda,

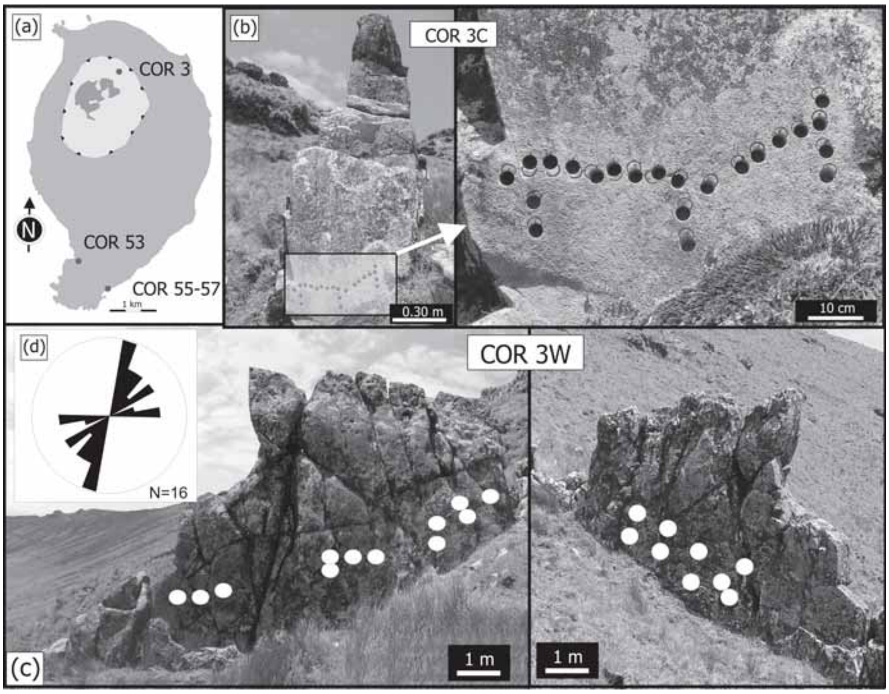

Fig. 2.- (a) Synthetic map with the location of the sampling sites. (b) Photographs correspon-ding to the sampled center part of the dyke COR3 (COR3C). (c) The sampled dike walls of site COR3 (COR3W). (d) Rose diagram corresponding to the orientation of mesoscopic dykes measured on field.

Fig. 2.- (a) Mapa sintético con la localización de los lugares de muestreo (b) Fotografías correspondiente a la zona central del dique COR3 (COR3C). (c) Paredes muestreadas del dique COR3 (COR3W). (d) Diagrama en rosa de los diques mesoscópicos medidos en el campo.

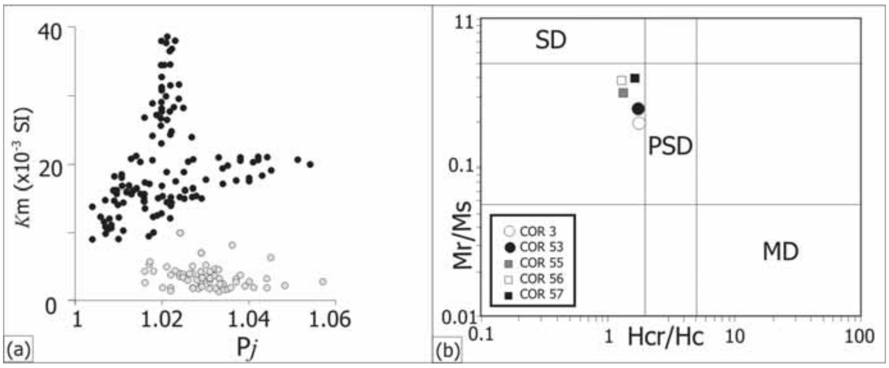

Fig. 3.- (a) P*j versus K*m plot. Open circles corresponding to the site COR3. Filled circles correspond to the rest of the sites. (b) The Day plot for representative samples coming from all the sites.

Fig. 3.- (a) Gráfico P*j *versus* K*m. Los círculos grises representan los datos de la estación COR3. Los círculos negros representan el resto de las estaciones. (b) Diagrama de Day de algunas muestras representativas de las estaciones realizadas.

1982; Rochette *et al.,* 1991; Callot *et al.,* 2001). On the other hand the magnetic parameters obtained from the hysteresis loops at room temperature (recorded for representative samples using a SQUID magnetometer, model MPMS-5S, Quantum Design) and geochemical analysis, indicate that the titanomagnetites are the main carrier of the magnetic susceptibility in these rocks. The correlation between the ratio of the coercivity of the remanence to the coercivity (Hcr/Hc) and the ratio of saturation remanence to saturation magnetisation (Mr/Ms) can be expressed in the Day plot (Fig. 3(b)). As shown, all the values for the analysed samples fit into the pseudo-single domain field. A certain diagonal trend, from the pseudo-single domain field to the single domain one occurrs, which can be interpreted as the result of a range of grain sizes (Borradaile and Werner, 1994).

Shape and orientation of the magnetic ellipsoids

The analysis of the shape of the magnetic ellipsoids was performed by means of anisotropy plots where the mean shape (T) corresponding to each site is plotted *versus* the degree of anisotropy (P*j*). As shown by the synthetic anisotropy plots (Fig. 4) a predominant triaxial shape characterizes the magnetic fabric of these samples (0.5>T>-0.5). The site mean values of the P*j* and T parameters vary from 1.01 to 1.04 and between +0.5 and -0.7 respectively. The very low degree of magnetic anisotropy (P*j* below 1.05) agrees with the values found in basaltic-andesitic shallow intrusive rocks (Hrouda, 1982; Staudigel *et al.*, 1992; Callot *et al.,* 2001) where titanomagnetite is the main carrier of the primary magnetic fabric and the AMS is controlled by the shape of the grains (shape anisotropy) and their alignment.

The directional analysis of the principal susceptibility axes for each site was performed by means of equal-area stereographic projections (Fig. 4). In all the cases, a good correlationship exists between the magnetic foliation (*K*1 and *K*2 axes) and the mean dyke wall. The mean of the *K*3 axes are perpendicular to the dyke wall, so these magnetic fabrics can be considered "normal magnetic fabrics" (Rochette *et al.,* 1991). This conclusion is also supported by the absence of single domain magnetites, which typically give rise to an "inverse magnetic fabric" (Rochette *et al*., 1992). Excluding the walls of the site COR3 (COR3W), in the rest of the sites, a well-developed magnetic lineation (grouping of the *K*1 axes) is defined. On site COR3, the samples located in the center of the dyke show a magnetic lineation in a vertical position (agrees with the orientation of piroxenes and plagioclase phenocrysts) and the magnetic ellipsoids have a prolate shape. On the contrary the pattern of the borders (COR3W) is characterized by a more foliated behaviour of the magnetic fabric (the magnetic foliation parallel to the mean dyke wall and predominant oblatened ellipsoids). In the rest of the sites (coming from the center to the dykes) the magnetic lineation is in a horizontal position (weakly dipping to the north) with predominant triaxial shapes of its magnetic ellipsoids.

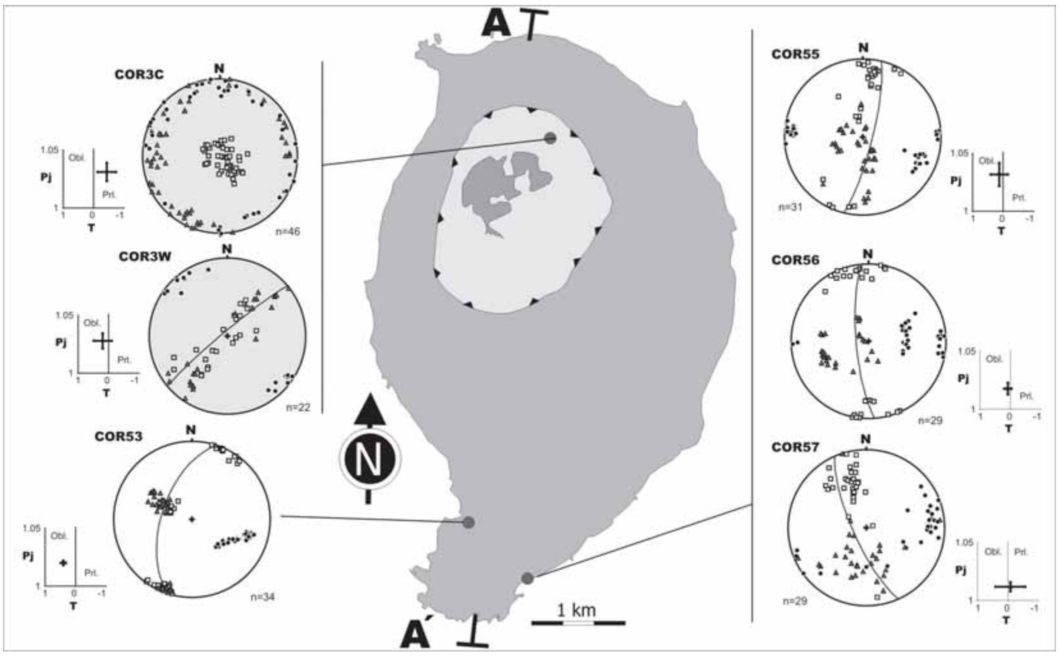

Fig. 4.- Stereoplots and anisotropy plots (P*j vs* T) for all the studied sites. Squares, triangles and circles, in the stereoplots, indicate *K*1, *K*2 and *K*3 directions respectively. The great circles represent the mean trend of the sampled dikes on each site.

Fig. 4.- Estereogramas y gráficos de anisotropía (P*j *vs* T) de las estaciones estudiadas. Los cuadrados, triángulos y círculos indican las direcciones de* K*1,* K*2 y* K*3 respectivamente. Las ciclográficas representan la dirección media de los diques muestreados en cada estación.

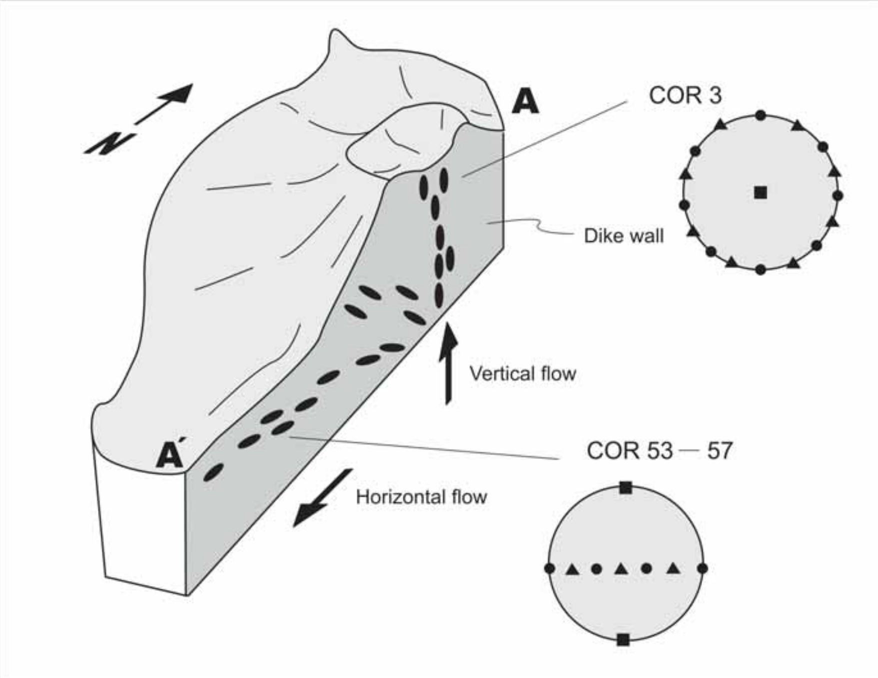

Fig. 5.- Synthetic sketch showing the relationship between the magnetic fabrics and its location within the Corvo volcanic complex.

Fig. 5.- Bloque diagrama sintético que muestra la relación entre las fábricas magnéticas y su localización en el complejo volcánico de la Isla de Corvo.

Discussion and conclusions

In accordance with Geoffroy *et al*. (2002), the flow vector in dykes can be calculated from their magnetic fabric using only the magnetic foliations. These authors state that, in vertical dykes, the flow vector can be defined completely by the intersection perpendicular to the axis between the magnetic foliation and the dyke wall. This is based on the symmetrical disposition of the magnetic foliations in relation to the shear effect near the dyke walls. Such a pattern has not been found in this study (see the close parallelism between the mean magnetic foliations on each side and with respect to the mean dyke wall in site COR3W, Fig. 4). Independently of the considered model in determining the flow direction (the orientation of the magnetic lineation or the imbrication of the magnetic foliations), the final interpretation must agrees with the petrostructural context.

From this point of view the whole of the studied magnetic fabrics are consistent with the position of the dykes within the volcanic complex. The magnetic fabric of site COR3 agrees with the vertical magma flow expected in the central part of the complex, which explains the observed mineral lineation (site COR3 in Fig. 5). On the contrary a N-S horizontal magma flow is expected to found far to the volcanic focus and then a horizontal magnetic lineation (sites COR53, 55, 56 and 57 in Fig. 5).

This preliminary study permits us to combine and compare the results of the AMS technique with those related to the petrostructural context to interpret the magma flow kinematics. The coherence between both magnetic and petrostructural data evidences that the orientation of the magnetic lineation can reflect the flow direction.

Acknowledgements

This work is a contribution to the “VULCMAC-Vulcanismo da Macaronésia” Project, code MAC/2.3/A7, financied by “Programa de Iniciativa Comunitaria INTERREG III B, Espaço Açores-Madeira-Canárias” and by “Direcçào Regional da Ciencia e Tecnología” of the Regional Government of Açores. Measurements of anisotropy of magnetic susceptibility were carried out at the Magnetic Fabrics Laboratory of the Earth Sciences Department (University of Zaragoza), using a susceptibility bridge Kappabridge KLY-3.

References

Azevedo, J.M.M., Alves, E.I. y Dias, J.L. (2003). Contributo para a interpretação vulcanostrutural da ilha do Corvo, Açores. *Ciências da Terra (UNL)*, Lisboa, nº esp.V, CD-ROM, A5-A8.

Borradaile, G. y Werner, T. (1994). *Tectonophysics*, 235, 223-248.

Callot, J.P. Geoffroy, L., Auborg, C., Pozzi, J.P. y Mege, D., 2001. *Tectonophysics*, 335, 313-329.

Cañón-Tapia, E., Walker, G.P.L. y Herrero-Bervera, E. (1996). *Journal of Volcanology and Geothermal Research*, 70, 21-36.

Ellwood, B.B., (1978). *Earth and Planetary Science Letters*, 41, 254-264.

Forjaz, V. H., (1988). Azores study tour. Field trip guide – *Anais do Seminar on the prediction of earthquakes*. ECEurope-UN, Lisbon. 26 p.

França, Z.T., Cruz, J.V., Nunes, J.C. y Forjaz, V.H. (2003). Geología dos Açores: Una perspectiva actual. *Açoreana*, 10 (1), 11-140.

Geoffroy, L., Callot, J.P., Aubourg, C. y Moreira, M. (2002). *Terra Nova*, 14, 183-190.

Herrero-Bervera, E., Cañón-Tapia, E., Walker, G.P.L. y Tanaka, H. (2001). *Journal of Volcanology and Geothermal Research*, 118, 161-171.

Hillhouse, J.W. y Wells, R.E. (1991). *Journal of Geophysical Research*, 96, 12443-12460.

Hrouda, F. (1982). *Geophysical Survey*, 5, 37-82.

Jelinek, V. (1981). *Tectonophysics*, 79, 63-67.

Knight, M.D. y Walker, G.P.L. (1988). *Journal of Geophisical Research*, 93, 4308-4319.

Rochette, P., Jenatton, L., Dupuy, C., Boudier, F. y Reuber, I. (1991). En: *Ophiolite Genesis and the Evolution of the Oceanic Lithosphere* (T.J. Peters, Ed.). Kluwer, Dordrecht, 55-82.

Rochette, P., Jackson, M. y Aubourg, C., (1992). *Reviews of Geophysics*, 30, 209-226.

Staudigel, H.G., Gee, G., Tauxe, L. y Varga, R.J. (1992). *Geology*, 20, 841-844.

Tarling, D.H. y Hrouda, F. (1993). *The magnetic anisotropy of rocks.* Chapman and Hall, London, 217p.